COMMUNICATIONS PHYSICS

ARTICLE

https://doi.org/10.1038/s42005-020-0297-3 OPEN

Control of electron recollision and molecular nonsequential double ionization

Shuai Li[1], Diego Sierra-Costa[1], Matthew J. Michie[1], Itzik Ben-Itzhak[2] & Marcos Dantus[1,3]✉

Intense laser pulses lasting a few optical cycles, are able to ionize molecules via different mechanisms. One such mechanism involves a process whereby within one optical period an electron tunnels away from the molecule, and is then accelerated and driven back as the laser field reverses its direction, colliding with the parent molecule and causing correlated non-sequential double ionization (NSDI). Here we report control over NSDI via spectral-phase pulse shaping of femtosecond laser pulses. The measurements are carried out on ethane molecules using shaped pulses. We find that the shaped pulses can enhance or suppress the yield of dications resulting from electron recollision by factors of 3 to 6. This type of shaped pulses is likely to impact all phenomena stemming from electron recollision processes induced by strong laser fields such as above threshold ionization, high harmonic generation, attosecond pulse generation, and laser-induced electron diffraction.

[1] Department of Chemistry, Michigan State University, East Lansing, MI 48824, USA. [2] J. R. Macdonald Laboratory, Department of Physics, Kansas State University, Manhattan, KS 66506, USA. [3] Department of Physics and Astronomy, Michigan State University, East Lansing, MI 48824, USA. ✉email: dantus@chemistry.msu.edu

Atomic ionization processes in the presence of strong laser fields are well modeled by single active electron ionization approximations at moderate intensities[1,2]. In contrast, non-sequential double ionization (NSDI) is complicated by strong electron correlation and Coulombic attraction to the ion core[3–5]. Processes analogous to those occurring in atoms take place in molecules, albeit with added complexity introduced by the presence of other atoms, molecular structure, additional degrees of freedom, and higher density of electronic states. Furthermore, unlike atoms, molecules, especially nonlinear polyatomic molecules, can experience electron recollision processes at any of their atoms, making possible the observation of NSDI with elliptical and even circularly polarized fields[6–14].

Understanding and controlling the behavior of molecules in strong fields requires the ability to discriminate between different double ionization mechanisms. The choice of a molecule with high ionization potential and long-wavelength short-pulse excitation has been shown to favor recollision-induced molecular NSDI[3]. Shorter wavelengths and longer pulse durations may cause NSDI in addition to sequential multiphoton ionization (MPI), wherein large fragment ions absorb additional photons from the field and undergo further fragmentation and ionization[15,16].

Controlling the ionization process would be useful to simplify the analysis of molecular ionization in strong fields. Moreover, controlling electron recollision could impact a wide range of phenomena that depend on this process, for example: molecular fragmentation, high-harmonic generation (HHG), the generation of attosecond pulses via HHG, above threshold ionization (ATI), and even attosecond clocking[5,17]. Control of these processes via pulse shaping has been of interest for over a decade[18]. Most relevant to the findings here are calculations that have shown that large effects can be gained by 'jumps' in the optical cycles of a pulse. For example, a pulse resulting from joining two identical pulses with one having its carrier envelope phase shifted by π, was predicted theoretically to extend the HHG cutoff[19]. Similarly, a theoretical exploration of pulses with an instantaneous π phase jump in the time domain predicted a significant extension of the HHG cutoff energy and the energies achieve by ATI[20,21]. Unfortunately, these schemes have not been experimentally implemented. The latter case, for example, would require pulses spanning more than five octaves, a capability that is well beyond the present state of the art in ultrafast science.

The purpose of the present study is to enhance or suppress the yield of metastable dications via spectral-phase pulse shaping. Inspired by the elegant control experiments by Silberberg using phase steps to control two-photon excitation[22], we use a phase step. However, in this work, laser-matter interactions are well outside the perturbation limit considered by Silberberg. In fact, perturbation theory only predicts a significant reduction in the yield of high-order (five photons or more) processes. The phase step in the frequency domain causes a jump in the time-dependent frequency of the pulse during the time when tunnel ionization and recollision occurs. The jump in frequency is relevant because recollision, NSDI, and HHG have been found to depend on the frequency of the laser elevated to a power of approximately five or eight[23–25], stemming from quantum path interferences with contribution from multiple returning orbits. In addition to calculations of the kinetic energy acquired by a free electron in the shaped laser field, we develop a model exclusively based on the fact that the frequency of the shaped pulses varies through the temporal pulse. Thus, we assume the position of the phase step with respect to the center frequency of the pulse and the sign of the phase step in the frequency domain is proportional to the frequency of the pulse at the times when recollision takes place.

Here, using laser pulses with identical spectrum and peak intensity, but different phase characteristics, we observe control over the yield of ions produced via NSDI and MPI mechanisms. We find that the model predicts quite closely the observed enhancement or suppression of dications as well as other electron recollision processes such as high-harmonic generation. We test the control mechanism using circularly polarized pulses, which involve longer orbits for the recolliding electron wavepacket and lower recollision energies. We find that the contrast observed for doubly charged fragment ions is slightly larger than that measured for linearly polarized pulses. This indicates that the control mechanism is associated either with the recolliding electron wavepacket orbit period, which is here manipulated by the position and sign of the phase step, or the kinetic energy of the recolliding electron, which is above or below the double ionization threshold due to pulse shaping. In summary, we report the observation of significant control over the yield of metastable dications as we scan a ¾π step across the spectrum of an intense femtosecond laser pulse. The enhancement or suppression of electron wavepacket recollision appears to be universal based on similar phase-step measurements, presented here, of the yield of helium double ionization and the intensity of gas-phase third harmonic generation.

Results

Conceptual background. Doubly charged ions, especially if metastable, are more likely to be formed by NSDI than by stepwise MPI. The goal of our experiments is to find if temporal shaping of the laser pulses can influence NSDI. The link between temporal shaping and electron recollision, which causes NSDI, is given by the kinetic energy of the electron which is accelerated by the electromagnetic field. Using shaped pulses with phase jumps in the time domain we thus seek to influence the orbit of the recolliding electron wavepacket and hence the probability for NSDI. Figure 1 illustrates how two different shaped pulses result in different electron recollision orbits, and thus different electron kinetic energies. Our goal is then to find shaped pulses for which a small change, such as a sign in the phase, causes the kinetic energy of the recolliding electron to be above or below threshold for NSDI.

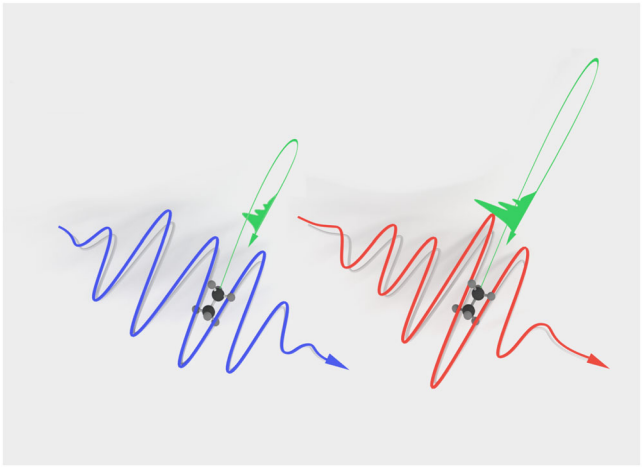

Fig. 1 Schematic representation of ethane molecules exposed to two different shaped laser pulses. The intense laser field (red and blue) drives an electron out of a sigma bond from the molecule through tunnel ionization accelerating away and then towards the molecule when the sign of the field changes. If the kinetic energy of the electron is sufficient to release the second electron it leads to the creation of metastable dications or, alternatively, the molecule undergoes multiphoton ionization during the subsequent optical cycles. We demonstrate that pulse shaping with a phase jump modifies the electric field and hence modifies the available electron kinetic energy. The position and sign of the phase jump thus control the nonsequential double ionization process and the resulting molecular fragments observed.

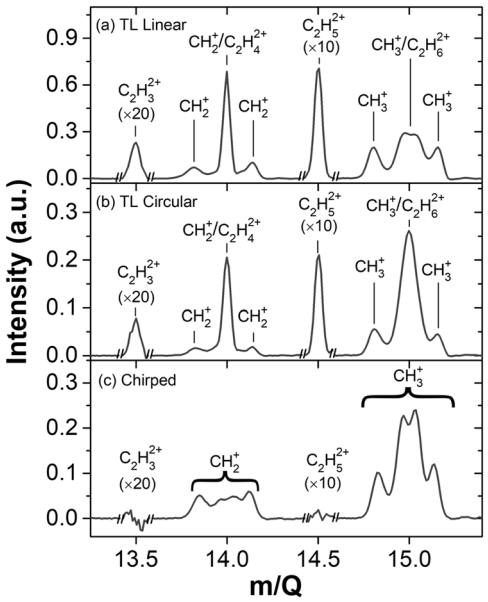

Fig. 2 Portion of the mass spectra of ethane obtained when using transform-limited (TL) 42 fs (**a**) linearly, (**b**) circularly polarized laser pulses, and (**c**) chirped pulses. At $m/Q = 14$ and 15 there is an overlap between singly charged CH_2^+ and CH_3^+ with doubly charged $C_2H_4^{2+}$ and $C_2H_6^{2+}$, respectively.

Table 1 Principal fragments and ions resulting from the strong field ionization of ethane.

Dissociative ionization of ethane: (appearance energies)		
Single ionization and fragmentation		
$C_2H_6 \rightarrow C_2H_6^+$	(11.56 eV)	Ref. [26]
$\rightarrow C_2H_5^+ + H$	(12.55 eV)	Ref. [29]
$\rightarrow C_2H_4^+ + H_2$	(11.81, 12.15 eV)	Ref. [8,26]
$\rightarrow C_2H_3^+ + H_2 + H$	(13.51, 14.8 eV)	Ref. [26,29]
$\rightarrow CH_3^+ + CH_3$	(13.65, 14.1 eV)	Ref. [26,29]
$\rightarrow CH_2^+ + CH_4$	(14.69 eV)	Ref. [26]
Double ionization and fragmentation		
$C_2H_6 \rightarrow C_2H_6^{2+}$	(32 ± 2 eV)	Ref. [29]
$\rightarrow C_2H_5^{2+} + H$	(32.3 eV)	Ref. [26]
$\rightarrow C_2H_4^{2+} + H_2$	(31–32 eV)	Estimated
$\rightarrow C_2H_3^{2+} + H_2 + H$	(35.5 eV)	Ref. [26]
$\rightarrow C_2H_5^+ + H^+$	(20.5 eV)	Ref. [29]
$\rightarrow C_2H_4^+ + H_2^+$	(18 eV)	Ref. [29]
$\rightarrow C_2H_3^+ + H_3^+$	(33.2 eV)	Ref. [29]
$\rightarrow CH_3^+ + CH_3^+$	(32 eV)	Ref. [29]
$\rightarrow 2CH_2^+ + H_2^+$	(28.55 eV)	Ref. [29]
Fragment ionization		
$CH_3 \rightarrow CH_3^+$	(9.84 eV)	Ref. [26]
$CH_2 \rightarrow CH_2^+$	(10.40 eV)	Ref. [26]
$H_2 \rightarrow H_2^+$	(15.43 eV)	Ref. [27]
$H \rightarrow H^+$	(13.60 eV)	Ref. [26]

The table was compiled from a number of previous photoionization, electron impact, and strong field studies[8,26–30]. The appearance energy, listed in brackets, for the ions and selected dissociation channels helps to determine pathways that follow direct double ionization, which requires more than 30 eV of total energy, and corresponds to direct formation of doubly charged metastable fragments. Ions with appearance energies below 16 eV correspond to single ionization or multiphoton dissociative ionization and fragmentation leading to multiple charged species.

Preliminary experiments. We irradiate isolated gas phase ethane molecules and collect the resulting ions using a time-of-flight (TOF) mass spectrometer. Figure 2 compares the region of the mass spectrum containing the fragment ions with mass to charge ratio (m/Q) between 13 and 15.5 obtained for ethane with 42-fs transform-limited (TL) 800-nm pulses that are either (a) linearly polarized, (b) circularly polarized, or (c) chirped to seven times their TL duration. The corresponding complete mass spectra are provided in Supplementary Figs. 1–3, and Table 1 has the appearance energy for most of the fragment ions observed in our measurement[8,26–30]. We note that the metastable dications fragments $C_2H_3^{2+}$, $C_2H_4^{2+}$, $C_2H_5^{2+}$, and $C_2H_6^{2+}$ are observed for both linear and circular polarization. In contrast, for chirped pulses, the yield of doubly charged ions is negligible. Note that for some species, such as $C_2H_4^{2+}$, the metastable doubly charged fragment ions may dissociate with a lifetime of hundreds of nanoseconds on their way to the detector[30]. In place of the relatively narrow peaks observed in Fig. 2a, b, one observes pairs of peaks in Fig. 2c. These split time of flight (TOF) peaks are associated with fragment-ion pairs due the Coulomb repulsion between the ion pairs, such as $CH_2^+ + CH_2^+$ and $CH_3^+ + CH_3^+$. Specifically, the peak pairs appear in the TOF spectra because some fragments are ejected toward the detector and thus arrive earlier, while others are ejected in the opposite direction and thus arrive later in time. The peak separation is proportional to the kinetic energy release resulting from the repulsion between positively charged ions. The appearance of Coulomb exploding ion pairs has been found to increase with pulse duration, in agreement with Fig. 2c. This supports the observation that longer pulses lead to the breakage of multiple bonds[31–33].

The peaks of the metastable dications $C_2H_3^{2+}$ and $C_2H_5^{2+}$ are easily identified by their unique half-mass unit position at m/Q of 13.5 and 14.5, respectively. The loss of three or one neutral hydrogen atoms, respectively, occurs with minimal kinetic energy such that these peaks are not broadened substantially. In contrast, both doubly and singly charged fragment ions can contribute to the TOF peaks at $m/Q = 14$ and 15. It is likely that the peak at $m/Q = 14$ has a significant contribution of the metastable $C_2H_4^{2+}$ dication, based on the fact that for linearly and circularly polarized light, the peak at $m/Q = 14$ is ten times larger than the peak at 14.5. Flanked by the peak at $m/Q = 14$ are the singly charged, $CH_2^+ + CH_2^+$ Coulomb explosion fragment-ion pairs. For chirped pulses, no doubly charged ions are detected and the single peak at $m/Q = 14$ becomes a double peak indicating Coulomb explosion among singly charged ion pairs. The chirped pulses are long enough to allow chemical bonds to lengthen and give rise to enhanced ionization[31]. A clear assignment cannot be made for $m/Q = 15$, therefore we shall focus the rest of our discussion on $C_2H_4^{2+}$ and $C_2H_5^{2+}$. The metastable fragment-ion $C_2H_3^{2+}$ has a lower yield, making it difficult to interpret quantitatively.

The data shown in Fig. 2a, b suggest that the double ionization mechanism observed for linear and for circular polarization is very similar, but different for chirped pulses. The Keldysh parameter γ,[34] helps identify the ionization regime by comparing the ionization potential of the atom or molecule to the cycle-averaged quiver energy of a free electron. When $\gamma < 1$, tunnel ionization can be considered to take place within an optical cycle of the pulse, whereas the regime when $\gamma > 1$ is known as the MPI regime. Based on the laser parameters and the ionization potential of ethane, NSDI is expected for 42-fs TL pulses linearly polarized $\{(3.0 \pm 0.5) \times 10^{14}\ \mathrm{W\,cm^{-2}},\ \gamma \sim 0.57,\ 3.2\mathrm{Up} \sim 57\ \mathrm{eV}\}$, and circularly polarized $\{(1.5 \pm 0.3) \times 10^{14}\ \mathrm{W\,cm^{-2}},\ \gamma \sim 0.8,\ 3.2\mathrm{Up} \sim 28\ \mathrm{eV}\}$, but not for chirped pulses $\{(0.56 \pm 0.10) \times 10^{14}\ \mathrm{W\,cm^{-2}},\ \gamma \sim 1.3,\ 3.2\mathrm{Up} \sim 11\ \mathrm{eV}\}$, for the latter MPI followed by fragmentation is anticipated given that $\gamma > 1$.

The metastable dications $C_2H_6^{2+}$; $C_2H_5^{2+}$; $C_2H_4^{2+}$ and $C_2H_3^{2+}$ result from NSDI based on the experimentally measured ellipticity dependence (see Supplementary Fig. 4), the observation

that $C_2H_6^{2+}$ exhibits the tale tell enhancement 'knee' of $Y(A^{++})/Y(A^{+})$ under linear and circularly polarized pulses[9]. The observation of high-order ATI of ethane; and supported by the observation of NSDI from a number of saturated and unsaturated hydrocarbons[9,11,12]. The sigma bonding electron is responsible for the initial tunnel ionization, leaving a weakly bound M^+, evidenced by its lower probability compared to $C_2H_5^+$ and $C_2H_4^+$, this results in a more pronounced yield of dications resulting from NSDI[6,8].

Early work on electron recollision in noble atoms led to the conclusion that field ellipticity prevents electron recollision[5,35]. It was assumed that NSDI, and the characteristic knee structure in the $Y(A^{++})/Y(A^{+})$ ratio associated with it, would similarly be suppressed in other systems exposed to elliptically-polarized fields. This assertion was contradicted soon after by the observation of NSDI under circularly polarized light in Mg atoms[7], and then by similar observations in NO, O_2[36], and ethane[9]. These observations are consistent with theoretical models and predictions[37]. The parameters required for an atom or molecule to exhibit NSDI have been summarized as a set of scaling laws and the presentation of a 'phase diagram' where it becomes clear that low ionization potential (below 13 eV for 800 nm laser pulses), and high peak intensity from relatively short pulses (20–50 fs) ensures the recolliding electron has sufficient energy to release the second electron[38–40]. Based on scaling laws proposed for photoelectrons, it has been possible to show the conditions under which one expects NSDI by circularly polarized light/pulses even for Ar and He atoms[40]. This conclusion is consistent with long recollision periodic orbits that are responsible for NSDI driven by circularly polarized light[37].

Results from shaped laser pulses. Figure 3 shows the corresponding portion of the mass spectrum for fragment ions of ethane with m/Q between 13 and 15.5 obtained with spectrally shaped laser pulses. The results shown in Fig. 3a have a positive ¾π phase step in either the high energy (blue line) or low energy (red-dashed line) portion of the spectrum. Notice that the yield of doubly charged fragments is greatly enhanced (suppressed) when the phase step is in the higher (lower) energy portion of the laser spectrum. The situation is reversed when a negative ¾π phase step is used, as shown in Fig. 3b. Note that the pairs of shaped pulses have identical spectra, energy, polarization, and peak intensity. The only difference is the location of the spectral-phase step. The reason why pulse shaping, as being carried out here, leads to such different strong-field ionization processes can be explained by considering that the frequency becomes time dependent, as described below.

Simulation of the experimental data. A sharp π phase step in the frequency domain results in a phase jump in the time domain that breaks the pulse into two pulses. For a given electric field in the frequency domain, given by

$$E(\omega) \equiv A(\omega)e^{i\varphi(\omega)} \propto \sqrt{I(\omega)}\, e^{i\varphi(\omega)}, \qquad (1)$$

where $A(\omega)$ is the amplitude and $\varphi(\omega)$ is the spectral phase, the shaped pulse in the time domain is obtained via the Fourier transformation

$$E(t) \equiv \frac{1}{2\pi}\int_{-\infty}^{+\infty} \sqrt{I(\omega)}\, e^{i\varphi(\omega)} e^{-i\omega t} \mathrm{d}\omega. \qquad (2)$$

Equations (1) and (2) can be used to obtain a time dependent description of the pulse $I(t) = |E(t)|^2$. The temporal shape of the pulse, given by $I(t)$, is identical for pairs of pulses with the same phase step sign and for which the position of the phase step in the frequency domain is detuned towards high/low energy

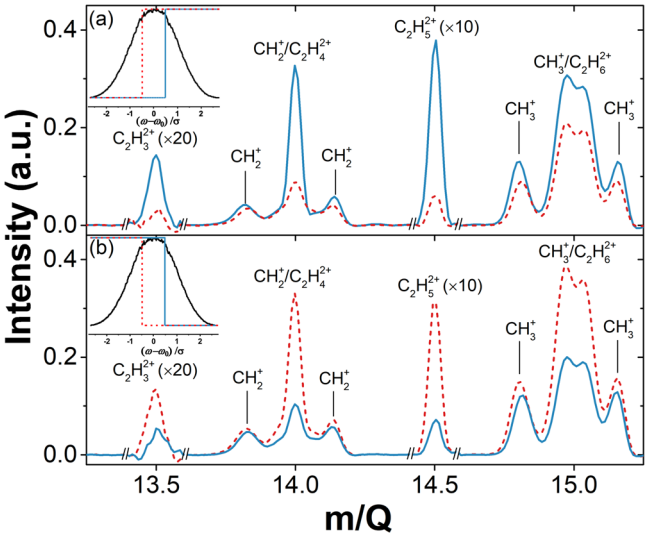

Fig. 3 Portion of the mass spectrum of ethane in the region showing the fragment ions with *m/Q* between 13 and 15.5 obtained using shaped pulses. a Laser spectra for two different shaped pulses with a positive ¾π phase step in either the high energy (blue line) or low energy (red-dashed line) portion of the laser spectrum (see inset diagrams showing their location at $\pm\sigma/2$ relative to ω_0). **b** Spectra for negative ¾π phase step in either the high energy (blue line) or low energy (red-dashed line) portion of the laser spectrum. Notice the phase step serves to enhance or suppress the yield of doubly charged fragment ions associated with non-sequential double ionization, and that the effect is reversed upon changing the sign of the phase step. The four spectra, shown as measured (without normalization), were obtained within the span of 30 min under identical conditions except for the frequency where the phase step is located.

symmetrically. We confirmed the shaped pulses were identical by comparing their second harmonic spectrum (Supplementary Fig. 5). Henceforth, we shall refer to these as "shaped-pulse pairs" that allow us to exclusively explore phase effects given that the pulses in the time domain are identical (see Supplementary Fig. 6). These types of pulses, with a positive or negative ¾π phase step, were employed in connection with control of the strong-field fragmentation of methanol[41]. The time-dependent intensity $I(t)$ of the pair of shaped pulses used to obtain the TOF spectra shown in Fig. 3a is identical and can be described as a small shoulder preceding the main pulse. Clearly, the differences observed in TOF spectra shown in Fig. 3a indicate that $I(t)$ alone is not responsible for the observed changes in fragment-ion yields. The position, magnitude, and sign of the phase step are the determining factors for the observed control over ionization. The same conclusions apply for the data shown in Fig. 3b, except that in this case $I(t)$ is reversed in time when compared to the pulses in Fig. 3a. For Fig. 3b, $I(t)$ can be described as a small shoulder following the main pulse.

Based on the aforementioned fifth- or sixth-order dependence of HHG on frequency[42,43], and the observed enhancement of NSDI by higher frequencies[25,44], we can assume that the difference in the yield of dications, observed here as an increase in the yield of doubly charged fragment ions, depends on the frequency of the field at the time of tunnel ionization. To simulate our data, we multiply the position of the phase step, expressed as $\omega - \omega_0$, where ω_0 is the central frequency of the pulse, by the spectrum of the pulse $I(\omega) = |E(\omega)|^2$ elevated to the n_{th} power given the nonlinearity of the process, where n is an odd number to maintain the sign dependence. Then, empirically we find that $n = 5$ fits the data better than $n = 7$. The fifth-order dependence is in agreement with the observed dependence of the

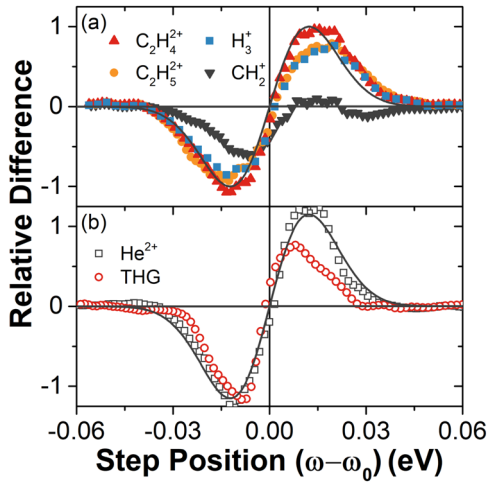

Fig. 4 Dependence of ion yields on the position of a ¾ π phase step. **a** Relative difference between measured ion yields of $C_2H_4^{2+}$, $C_2H_5^{2+}$, and H_3^+, which are associated with non-sequential double ionization, as well as CH_2^+ Coulomb explosion fragment. **b** Relative difference between measured yield for doubly charged He and third harmonic generation (THG) photon yield in air for pulses similarly shaped as for the data in panel (**a**). The thin black line shown in both panels (**a**) and (**b**) corresponds to our phenomenological model, i.e. $(\omega-\omega_0)I^5(\omega-\omega_0)$, and the measured relative difference is shown "as measured" without normalization. Error bars, defined as the standard deviation of integrated ion count, are within the symbol size.

ion yield on laser pulse intensity (linearly polarized) observed for Xe^+ and C_{60}^+[45]. The product $(\omega-\omega_0)I^5(\omega-\omega_0)$ is plotted in Fig. 4a, b (solid line) as a function of the phase step position together with the relative difference (defined below) in the yield of ions. The 'instantaneous frequency'[46], describes how the frequency of the pulse changes as a function of time

$$\omega_{\mathrm{inst}}(t) \equiv \omega_0 + \frac{\mathrm{d}\{\mathrm{Im}[\ln[E(t)]]\}}{\mathrm{d}t}, \qquad (3)$$

where ω_0 is the carrier frequency of the pulse, and the expression in the curly brackets corresponds to the time dependent phase of the pulse. This instantaneous frequency combines both frequency and time domains and can be unreliable when sharp changes in either frequency or time occur. Nevertheless, we calculated $\omega_{\mathrm{inst}}(t)$ when $I(t)$ approaches its maximum amplitude. We then multiplied it by $I^5(\omega-\omega_0)$ and obtained a function that is very similar to that plotted in Fig. 4a, allowing us to justify simply using the position of the phase step as a simple phenomenological model of the observed results.

In order to test this phenomenological model, we acquired TOF spectra as a function of the position of a ¾π phase step with respect to the center of the spectrum $\omega-\omega_0$, for both positive and negative phase steps. The results were plotted as the relative difference, a quantity that expresses the difference between two ion yields normalized by the average of the two, specifically $(Y^+-Y^-)/[(Y^++Y^-)/2]$, where the superscript sign indicates that the yield is measured for either a positive or negative phase step. For example, when the yield of some ion for a positive phase is three times greater than the yield for a negative phase at the same phase position, then the relative difference at that position is 1.0.

We find that the relative difference for doubly charged, $C_2H_4^{2+}$ and $C_2H_5^{2+}$, fragment ions is in very good agreement with the model (thin black line). Interestingly, H_3^+, a minor fragment ion resulting from double ionization of ethane[30,47], follows the same trend, see Fig. 4a. In alcohols, NSDI most likely involves the non-bonding electrons at the oxygen atom, causes a reduction in electron density from the nearest carbon atom and leads to formation of neutral H_2, which roams and extracts an additional proton to produce H_3^+[48,49]. Apparently, a similar process occurs in ethane. This observation is consistent with experiments on CH_3CD_3 for which the yields of H_2^+ and D_2^+ amounted to 93% of the diatomic ions, and the yields of H_2D^+ and HD_2^+ amounts to 65% of the triatomic ions and the rest to H_3^+ and D_3^+[30]. The yield for Coulomb explosion CH_2^+ ions, also shown in Fig. 3a, identified as shoulders flanking the $m/Q=14$ peak, are found to have a weaker dependence on the phase step. Note that in Fig. 3a, b the amplitude of the CH_2^+ fragment ion is less affected by the position or sign of the phase step than the $C_2H_4^{2+}$ ions.

The agreement between the model and experiment in Fig. 4 suggests that the control mechanism is related to the position of the phase step, which causes a change in the instantaneous frequency and hence the period of the optical cycle of the pulse at the time of tunnel ionization. We observe maximum differences for step positions ±0.015 eV relative to the photon energy 1.55 eV. The pulses used are well described by a Gaussian function and the step position corresponds to ±σ/2 relative to ω_0, where the intensity of the pulse is reduced by 1/e at ±σ. Because in each pulse pair we compare symmetric blue and red shifted frequency positions, the change in frequency is ~0.03 eV. While this difference seems to be small, as pointed above, recollision, NSDI, and HHG have been found to depend on the frequency of the pulse to the fifth or sixth power[23–25]. In terms of the frequency difference, we would anticipate a ~23% relative difference in the yield $I^6(\omega_{\mathrm{blue}})-I^6(\omega_{\mathrm{red}})$ divided by the average of those quantities. This estimate is much smaller than the experimentally achieved control factor of three. Possible reasons for the much greater control achieved include the fact that multiple returning orbits of the electron can cause NSDI, and the experiments are carried out near the threshold for highly nonlinear processes; requiring 11.5 eV for first ionization (equivalent to 8 photons), and 32 ± 2 eV (equivalent to 21 photons) for double ionization. Note that the appearance energy of doubly charged fragment ions and H_3^+ fragment ions following ethane double ionization is 33 ± 1 eV (equivalent to 21 photons)[28,29]. Preliminary one-dimensional kinetic energy calculations for an unbound electron in the presence of the shaped laser field based on classical mechanics were carried out. An electron with mass m at rest interacting with a strong laser field $E(t)$ experiences a force that is proportional to the electric field. Therefore, the kinetic energy of the electron at time τ is given by $E_{\mathrm{kin}}(\tau)=(1/2)m(-\int_{t_i}^{\tau}E(t)\mathrm{d}t)^2$. The results from those calculations are shown in Supplementary Fig. 7. We hope that our results will motivate theorists to simulate our observations with more advanced methods.

Results from shaped circularly polarized laser pulses. Based on recent simulations aimed at understanding the observed NSDI from Mg atoms[7,10,37,50–55] and some molecules[45,56–61], circularly polarized pulses are associated with orbits having longer recollision times. These findings allow us to test our hypothesis that the observed control over the yield of doubly charged ions is caused by the instantaneous frequency at the time of ionization. Although longer orbits will lead to greater electron wavepacket dispersion, for a given orbit, higher frequencies imply shorter periods and less time for electron wavepacket dispersion. Therefore, longer recollision orbits should be even more sensitive to changes in instantaneous frequency of the shaped pulses.

Figure 5 shows the mass spectrum of ethane fragment ions with m/Q between 13 and 15.5 obtained with spectrally shaped laser pulses that were circularly polarized. A reduction in overall yield of all ions was found upon changing the polarization of the pulses given that the laser pulse energy was kept constant, and

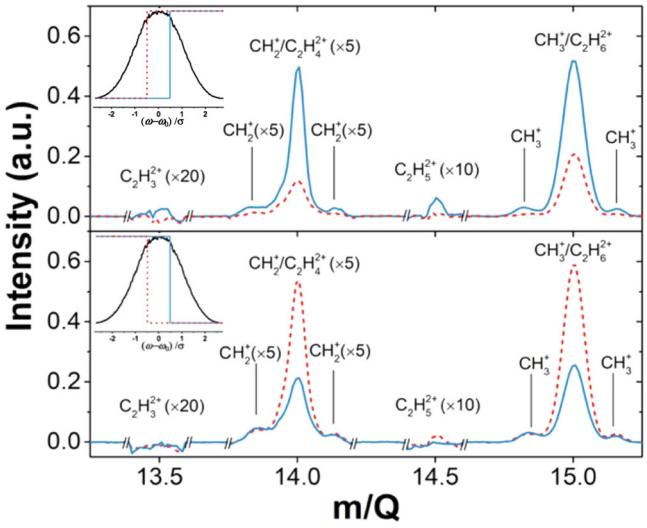

Fig. 5 Portion of the mass spectrum of ethane in region showing the fragment ions with *m/Q* between 13 and 15.5 obtained using shaped circularly polarized pulses. a Results for a positive ¾π phase step in either the high energy (blue line) or low energy (red-dashed line) portion of the laser spectrum (see inset diagrams showing their location at ±σ/2 relative to ω_0). **b** Spectra for negative ¾π phase step in either the high energy (blue line) or low energy (red-dashed line) portion of the laser spectrum. Notice the phase step serves to enhance or suppress doubly charged fragment ions associated with non-sequential double ionization, and that the effect is reversed upon changing the sign of the phase step. The four spectra were obtained under identical conditions, except for the phase step location. The data is shown as measured without normalization.

thus the peak intensity was reduced by a factor of 2 (recall that the peak field for circularly polarized pulses is decreased by √2 compared to linearly polarized pulses). The yield of dications for circularly polarized light was only 10% of that found for linearly polarized light. The ion yield dependence on polarization ellipticity is included in (Supplementary Fig. 4). We focus our analysis on the difference (blue/red lines) observed for the doubly charged $C_2H_4^{2+}$ and $C_2H_5^{2+}$, ions which is ~3 and >10, respectively, as determined by integrating the respective peaks in the TOF spectra. These ratios are contrasted with those observed for linearly polarized pulses, which are ~2 and ~6, respectively. The ~50% greater contrast observed for circularly polarized light seems to be consistent with the hypothesis that longer orbits are more sensitive to changes in the driving frequency. Note, these ratios are obtained from Figs. 3 and 5, and are not the relative differences shown in Fig. 4, which compare positive and negative phases at a given phase-step position. The lower contrast observed for $C_2H_4^{2+}$ indicates that this peak has a contribution of CH_2^+ fragment ions paired with neutral counterparts[30]. We note that, as in Fig. 3, the yield for the CH_2^+ Coulomb explosion channel is less affected by pulse shaping. We find that in the case of ethane, Coulomb explosion fragment ions are more prevalent than doubly charged fragments when linearly chirped pulses are used, see Fig. 2c.

Considerations for future experiments. The degree of control reported here, a factor of three to six (corresponding to relative differences of 1–1.4) in the yield of doubly charged fragments resulting from pulse shaping, warrants extensive scrutiny. The explanation given is based on the chirp rate at the time of double ionization, albeit taking into consideration multiple electron orbits being accelerated by a few optical cycles. We tested the generality of the recollision control obtained by ¾π phase step shaped pulses and found that the yield of He^{2+} and of third harmonic generation in air have a similar dependence on the observed yield of ethane dications found here, see Fig. 3(b). Furthermore, our findings are consistent with enhanced H_3^+ formation from methanol observed under similar experimental conditions[41]. Further confirmation using shorter pulses, where the greater bandwidth will allow a greater frequency change, will be valuable. Electron correlation measurements[62] will help provide a definite assignment of the NSDI process; in particular, if it is associated with recollision excitation followed by double ionization (RESI) or recollision-induced ionization (RII)[13,62]. Future experiments capable of detecting the momenta of the two electrons and the associated ions in coincidence, may help further identify NSDI dissociative pathways. Such a task is very demanding given that in some of the channels of interest there is a neural fragment or overlapping competing processes. Moreover, unlike photodissociation experiments carried out with single photon, the amount of energy (i.e., number of photons) absorbed by the molecule from the strong field used in this experiment is unknown. Simulations based on simpler systems, such as helium could also shed light on the role of the shaped pulses. Finally, other pulse shaping approaches may yield even greater changes in frequency while maintaining short-pulse duration, and therefore may lead to even higher level of control. For example, we have found that a very small (almost unmeasurable) chirp, causing <1.005 times pulse broadening, affects the control observed (see Supplementary Fig. 8). Comparison with recent methods aimed at tailoring the excitation field via the addition of other frequencies will also be instructive[63].

Discussion

We found that scanning the position of a ¾π phase step across the spectrum of an intense femtosecond laser pulse leads to significant (factors of 3–6) changes in the yield of doubly charged fragment ions, as well as fragment ions associated with NSDI. A phenomenological model based on the position of the phase step relative to the central frequency of the pulse was found to be in excellent agreement with the experimental results. We found the maximum degree of control, enhancement/suppression of doubly charged species, is observed when the phase step is near ±σ/2 of the Gaussian laser spectrum. We experimentally confirmed the general ability of ¾π phase step shaped pulses to control electron recollision by quantifying the yield of metastable dications from ethane, as well as for double ionization of helium and third harmonic generation in air. Finally, we found that the degree of control increased for ethane under circularly polarized laser pulses. All processes that depend on electron recollision, such as HHG, generation of attosecond pulses via HHG, ATI, attochirp measurements, and attosecond clocking, should thus be controllable by tailoring the phase of the incident femtosecond laser pulses as indicated here without the need for adding pulses with different frequencies.

We predict that the magnitude of the control reported here using shaped pulses will increase as the duration of the laser pulses decreases. Methods to introduce a phase step causing minimum or no loss[64] of pulse energy could represent significant enhancements in harmonic generation intensities, modest gains in cutoff energies, and significant increases in ATI yields. In terms of molecular processes, this type of pulse shaping could enable the double ionization of non-bonding electron pairs within a molecule, given the fact that linearly polarized light will favor electron recollision back to the orbital from which the electron tunnel ionized[17,65]. This degree of localized double ionization, as opposed to ionization out of delocalized valence orbitals,

involving for example oxygen and nitrogen atoms, could allow unprecedented control of chemical reactivity, such as being able to cleave strong chemical bonds and not neighboring weaker bonds[66].

Methods

Experiments are carried out employing a Wiley-McLaren TOF mass spectrometer operated at 10^{-7} Torr. The laser pulses are generated by a 1 kHz titanium sapphire chirped pulse amplified regenerative amplifier and attenuated to achieve the desired intensities (between 0.2 and 0.5 mJ per pulse). The pulses are first compressed to within 99.9% of the theoretical transform limit (40 fs), eliminating higher order dispersion, using the multiphoton intrapulse interference phase scan (MIIPS) method[67,68], and then shaped using a commercial pulse shaper (model MIIPS-HD, Biophotonic Solutions, now part of IPG Photonics). Achieving pairs of shaped pulses that agree with theoretical predictions based on the second harmonic spectrum of the shaped pulses (see Supplementary Fig. 4)[69] required using TL pulses with <40-fs^2 of chirp and no measurable high-order dispersion. The compressed pulses are focused into the chamber by an achromatic 300 mm focal length lens. Peak intensities are calibrated in situ by comparing the ratio between singly and doubly charged oxygen, nitrogen, and argon with experimental values reported in the literature[36,70]. The reported peak intensities are accurate within ~20%. Ions formed by the laser pulse are detected using a microchannel plate, the resulting TOF spectrum was then digitized. Background electronic noise signature from the laser was acquired while the laser was blocked and subtracted from the raw time-of flight transients. Ion yields are obtained by integrating the appropriate peaks in the TOF spectrum. The mass spectra in Figs. 2, 3 and 5 are averages of 100,000 pulses, and the mass to charge range shown is obtained from 205 TOF points which are converted to m/Q. The data points in Fig. 4 represent averaged integrated intensity for each ion shown from 5000 laser pulses for each phase step position. Each such scan consisted of 200 phase step positions. To avoid overlapping of multiple traces, only half of the points are shown after 3-point smoothing of the original scans (for H_3^+ we only show one quarter of the points obtained). The results for He were obtained using 40 fs TL pulses with a peak intensity of 6×10^{14} W cm^{-2}.

Data availability

The data that support the findings of this study are available from the corresponding author upon reasonable request.

Received: 3 July 2019; Accepted: 20 January 2020;
Published online: 13 February 2020

References

1. l'Huillier, A., Lompre, L. A., Mainfray, G. & Manus, C. Multiply charged ions induced by multiphoton absorption in rare gases at 0.53 μm. *Phys. Rev. A* **27**, 2503–2512 (1983).
2. Ammosov, M. V., Delone, N. B. & Krainov, V. P. Tunnel ionization of complex atoms and of atomic ions in an alternating electromagnetic field. *JEPT* **91**, 2008–2013 (1986).
3. Bhardwaj, V. R., Rayner, D. M., Villeneuve, D. M. & Corkum, P. B. Quantum interference in double ionization and fragmentation of C_6H_6 in intense laser fields. *Phys. Rev. Lett.* **87**, 253003 (2001).
4. Yudin, G. L. & Ivanov, M. Y. Physics of correlated double ionization of atoms in intense laser fields: quasistatic tunneling limit. *Phys. Rev. A* **63**, 033404 (2001).
5. Corkum, P. B. Plasma perspective on strong field multiphoton ionization. *Phys. Rev. Lett.* **71**, 1994–1997 (1993).
6. Cornaggia, C. & Hering, P. Nonsequential double ionization of small molecules induced by a femtosecond laser field. *Phys. Rev. A* **62**, 23403 (2000).
7. Gillen, G. D., Walker, M. A. & Van Woerkom, L. D. Enhanced double ionization with circularly polarized light. *Phys. Rev. A* **64**, 043413 (2001).
8. Li, W. et al. Dissociative photoionization dynamics in ethane studied by velocity map imaging. *Chem. Phys. Lett.* **374**, 334–340 (2003).
9. Ma, R. et al. Double ionization of C_2H_4 and C_2H_6 molecules irradiated by an intense femtosecond laser field. *Chem. Phys. Lett.* **404**, 370–373 (2005).
10. Mauger, F., Chandre, C. & Uzer, T. Recollisions and correlated double ionization with circularly polarized light. *Phys. Rev. Lett.* **105**, 083002 (2010).
11. Sharifi, S. M., Talebpour, A. & Chin, S. L. Double ionization of unsaturated hydrocarbons interacting with high-power femtosecond laser pulses. *J. At. Mol. Opt. Phys.* **2009**, 573020 (2010).
12. Xie, X. et al. Attosecond-recollision-controlled selective fragmentation of polyatomic molecules. *Phys. Rev. Lett.* **109**, 243001 (2012).
13. Becker, W., Liu, X., Ho, P. J. & Eberly, J. H. Theories of photoelectron correlation in laser-driven multiple atomic ionization. *Rev. Mod. Phys.* **84**, 1011–1043 (2012).
14. Wang, C. et al. Electron-ion differential cross section extracting from the high-order above-threshold ionization spectroscopy of C_2H_4 and C_2H_6. *J. Phys.: Conf. Ser.* **488**, 32041 (2014).
15. Müller, A. M., Uiterwaal, C. J. G. J., Witzel, B., Wanner, J. & Kompa, K.-L. Photoionization and photofragmentation of gaseous toluene using 80-fs, 800-nm laser pulses. *J. Chem. Phys.* **112**, 9289–9300 (2000).
16. Konar, A. et al. Polyatomic molecules under intense femtosecond laser irradiation. *J. Phys. Chem. A* **118**, 11433–11450 (2014).
17. Brabec, T. & Krausz, F. Intense few-cycle laser fields: Frontiers of nonlinear optics. *Rev. Mod. Phys.* **72**, 545–591 (2000).
18. Winterfeldt, C., Spielmann, C. & Gerber, G. *Colloquium*: optimal control of high-harmonic generation. *Rev. Mod. Phys.* **80**, 117–140 (2008).
19. Pérez-Hernández, J. A. et al. Extension of the cut-off in high-harmonic generation using two delayed pulses of the same colour. *J. Phys. B . Mol. Opt. Phys.* **42**, 134004 (2009).
20. Hu, P., Niu, Y., Xiang, Y. & Gong, S. Above-threshold ionization by few-cycle phase jump pulses. *Opt. Express* **21**, 24309 (2013).
21. Shan, B. & Chang, Z. Dramatic extension of the high-order harmonic cutoff by using a long-wavelength driving field. *Phys. Rev. A* **65**, 011804 (2001).
22. Meshulach, D. & Silberberg, Y. Coherent quantum control of multiphoton transitions by shaped ultrashort optical pulses. *Phys. Rev. A* **60**, 1287–1292 (1999).
23. Tate, J. et al. Scaling of wave-packet dynamics in an intense midinfrared field. *Phys. Rev. Lett.* **98**, 013901 (2007).
24. Frolov, M. V., Manakov, N. L. & Starace, A. F. Wavelength scaling of high-harmonic yield: threshold phenomena and bound state symmetry dependence. *Phys. Rev. Lett.* **100**, 173001 (2008).
25. Wang, Y. et al. Wavelength scaling of atomic nonsequential double ionization in intense laser fields. *Phys. Rev. A* **95**, 063415 (2017).
26. Plessis, P. & Marmet, P. Electroionization study of ethane: ionization and appearance energies, ion-pair formations and negative ions. *Can. J. Chem.* **65**, 1424–1432 (1987).
27. Shiner, D., Gilligan, J. M., Cook, B. M. & Lichten, W. H_2, D_2, and HD ionization potentials by accurate calibration of several iodine lines. *Phys. Rev. A* **47**, 4042–4045 (1993).
28. Au, J. W., Cooper, G. & Brion, C. E. The molecular and dissociative photoionization of ethane, propane, and n-butane: absolute oscillator strengths (10–80 eV) and breakdown pathways. *Chem. Phys.* **173**, 241–265 (1993).
29. Tian, C. & Vidal, C. R. Electron impact dissociative ionization of ethane: cross sections, appearance potentials, and dissociation pathways. *J. Chem. Phys.* **109**, 1704–1712 (1998).
30. Hoshina, K., Kawamura, H., Tsuge, M., Tamiya, M. & Ishiguro, M. Metastable decomposition and hydrogen migration of ethane dication produced in an intense femtosecond near-infrared laser field. *J. Chem. Phys.* **134**, 064324 (2011).
31. Bandrauk, A. D., Chelkowski, S. & Kawata, I. Molecular above-threshold-ionization spectra: the effect of moving nuclei. *Phys. Rev. A* **67**, 013407 (2003).
32. Lozovoy, V. V. et al. Control of molecular fragmentation using shaped femtosecond pulses. *J. Phys. Chem. A* **112**, 3789–3812 (2008).
33. Xie, X. et al. Duration of an intense laser pulse can determine the breakage of multiple chemical bonds. *Sci. Rep.* **5**, 12877 (2015).
34. Keldysh, L. V. Ionization in the field of a strong electromagnetic wave. *J. Exp. Theor. Phys.* **47**, 1945 (1965).
35. Krause, J. L., Schafer, K. J. & Kulander, K. C. High-order harmonic generation from atoms and ions in the high intensity regime. *Phys. Rev. Lett.* **68**, 3535–3538 (1992).
36. Guo, C., Li, M., Nibarger, J. P. & Gibson, G. N. Single and double ionization of diatomic molecules in strong laser fields. *Phys. Rev. A* **58**, R4271–R4274 (1998).
37. Wang, X. & Eberly, J. H. Nonadiabatic theory of strong-field atomic effects under elliptical polarization. *J. Chem. Phys.* **137**, 22A542 (2012).
38. Fu, L. B., Xin, G. G., Ye, D. F. & Liu, J. Recollision dynamics and phase diagram for nonsequential double ionization with circularly polarized laser fields. *Phys. Rev. Lett.* **108**, 103601 (2012).
39. Dong, S., Zhang, Z., Bai, L. & Zhang, J. Scaling law of nonsequential double ionization. *Phys. Rev. A* **92**, 33409 (2015).
40. Chen, X., Wu, Y. & Zhang, J. Knee structure in double ionization of noble atoms in circularly polarized laser fields. *Phys. Rev. A* **95**, 013402 (2017).
41. Michie, M. J., Ekanayake, N., Weingartz, N. P., Stamm, J. & Dantus, M. Quantum coherent control of H_3^+ formation in strong fields. *J. Chem. Phys.* **150**, 044303 (2019).
42. Schiessl, K., Ishikawa, K. L., Persson, E. & Burgdörfer, J. Quantum path interference in the wavelength dependence of high-harmonic generation. *Phys. Rev. Lett.* **99**, 253903 (2007).
43. Emelina, A. S., Emelin, M. Y. & Ryabikin, M. Y. Wavelength scaling laws for high-order harmonic yield from atoms driven by mid- and long-wave infrared laser fields. *J. Opt. Soc. Am. B* **36**, 3236–3245 (2019).

44. Milošević, D. B. et al. Wavelength dependence of channel-closing enhancements in high-order above-threshold ionization and harmonic generation. *J. Mod. Opt.* **55**, 2653–2663 (2008).
45. Hertel, I. V. et al. Fragmentation and ionization dynamics of C_{60} in elliptically polarized femtosecond laser fields. *Phys. Rev. Lett.* **102**, 023003 (2009).
46. Siegman, A. E. *Lasers*. (University Science Books, Mill Valley, CA, 1986).
47. Hoshina, K., Furukawa, Y., Okino, T. & Yamanouchi, K. Efficient ejection of H3+ from hydrocarbon molecules induced by ultrashort intense laser fields. *J. Chem. Phys.* **129**, 104302 (2008).
48. Ekanayake, N. et al. Mechanisms and time-resolved dynamics for trihydrogen cation (H3+) formation from organic molecules in strong laser fields. *Sci. Rep.* **7**, 4703 (2017).
49. Ekanayake, N. et al. H_2 roaming chemistry and the formation of H_3^+ from organic molecules in strong laser fields. *Nat. Commun.* **9**, 5186 (2018).
50. Shvetsov-Shilovski, N. I., Goreslavski, S. P., Popruzhenko, S. V. & Becker, W. Ellipticity effects and the contributions of long orbits in nonsequential double ionization of atoms. *Phys. Rev. A* **77**, 063405 (2008).
51. Wang, X. & Eberly, J. H. Elliptical trajectories in nonsequential double ionization. *N. J. Phys.* **12**, 093047 (2010).
52. Tong, A., Zhou, Y., Huang, C. & Lu, P. Electron dynamics of molecular double ionization by circularly polarized laser pulses. *J. Chem. Phys.* **139**, 074308 (2013).
53. Kamor, A., Mauger, F., Chandre, C. & Uzer, T. How key periodic orbits drive recollisions in a circularly polarized laser field. *Phys. Rev. Lett.* **110**, 253002 (2013).
54. Yuan, K.-J., Lu, H. & Bandrauk, A. D. High-order-harmonic generation in molecular sequential double ionization by intense circularly polarized laser pulses. *Phys. Rev. A* **92**, 023415 (2015).
55. Xu, T.-T. et al. Temporal correlation and correlated momentum distribution in nonsequential double ionization of Mg by circularly polarized laser fields. *Laser Phys.* **27**, 075301 (2017).
56. Zuo, W. et al. Experimental and theoretical study on nonsequential double ionization of carbon disulfide in strong near-IR laser fields. *Phys. Rev. A* **93**, 053402 (2016).
57. Gong, X. et al. Ellipticity dependent symmetric break of doubly ionized acetylene in strong laser fields. *J. Opt.* **19**, 124008 (2017).
58. Xu, H. et al. Effect of laser parameters on ultrafast hydrogen migration in methanol studied by coincidence momentum imaging. *J. Phys. Chem. A* **116**, 2686–2690 (2012).
59. Zhang, L. et al. Path-selective investigation of intense laser-pulse-induced fragmentation dynamics in triply charged 1,3-butadiene. *J. Phys. B At. Mol. Opt. Phys.* **45**, 085603 (2012).
60. Atia-tul-noor et al. Ellipticity-dependent fragmentation of acetylene dications. *Phys. Rev. A* **97**, 033402 (2018).
61. Zhao, A., Sándor, P., Tagliamonti, V., Matsika, S. & Weinacht, T. Molecular double ionization using strong field few-cycle laser pulses. *J. Phys. Chem. A* **120**, 3233–3240 (2016).
62. Kang, H., Zhou, Y. & Lu, P. Steering electron correlation time by elliptically polarized femtosecond laser pulses. *Opt. Express* **26**, 33400 (2018).
63. Bruner, B. D. et al. Robust enhancement of high harmonic generation via attosecond control of ionization. *Opt. Express* **26**, 9310 (2018).
64. Pastirk, I., Resan, B., Fry, A., MacKay, J. & Dantus, M. No loss spectral phase correction and arbitrary phase shaping of regeneratively amplified femtosecond pulses using MIIPS. *Opt. Express* **14**, 9537 (2006).
65. Corkum, P. B. & Krausz, F. Attosecond science. *Nat. Phys.* **3**, 381–387 (2007).
66. Kalcic, C. L., Gunaratne, T. C., Jones, A. D., Dantus, M. & Reid, G. E. Femtosecond laser-induced ionization/dissociation of protonated peptides. *J. Am. Chem. Soc.* **131**, 940–942 (2009).
67. Xu, B. et al. Quantitative investigation of the multiphoton intrapulse interference phase scan method for simultaneous phase measurement and compensation of femtosecond laser pulses. *J. Opt. Soc. Am. B* **23**, 750 (2006).
68. Coello, Y. et al. Interference without an interferometer: a different approach to measuring, compressing, and shaping ultrashort laser pulses. *J. Opt. Soc. Am. B* **25**, A140–A150 (2008).
69. Lozovoy, V. V., Pastirk, I., Walowicz, K. A. & Dantus, M. Multiphoton intrapulse interference. II. Control of two- and three-photon laser induced fluorescence with shaped pulses. *J. Chem. Phys.* **118**, 3187–3196 (2003).
70. Weber, T. et al. Sequential and nonsequential contributions to double ionization in strong laser fields. *J. Phys. B At. Mol. Opt. Phys.* **33**, L127–L133 (2000).

Acknowledgements

This material is based upon work supported by the U.S. Department of Energy, Office of Science, Office of Basic Energy Sciences, Atomic, Molecular and Optical Sciences Program under Award Number SISGR (DE-SC0002325). I.B-I. acknowledges support from the same funding agency under Award Number DE-FG02-86ER13491. The authors acknowledge insightful discussions with Anthony F. Starace, Robert R. Jones, J.E. Jackson, Ben Levine, and Travis Severt. We would like to dedicate this article to the late Professor Yaron Silberberg who inspired generations of physicists with elegant experiments, many of which involve phase steps being scanned across the spectrum of femtosecond laser pulses.

Author contributions

S.L., D.S.-C., and M.J.M. setup and performed the time-of-flight experiments, analyzed data, and prepared figures. Many valuable insights and suggestions were provided by I.B.-I. M.D. conceived the project, analyzed data, performed calculations, modeled the results, and supervised the project. S.L., I.B-I. and M.D. participated in the scientific discussions and in the revisions of the final manuscript.

Competing interests

The authors declare no competing interests.

Additional information

Supplementary information is available for this paper at https://doi.org/10.1038/s42005-020-0297-3.

Correspondence and requests for materials should be addressed to M.D.

Reprints and permission information is available at http://www.nature.com/reprints

Publisher's note Springer Nature remains neutral with regard to jurisdictional claims in published maps and institutional affiliations.